Supplementary Materials
Excitation Energies in a Polarizable Environment: A Comparison of State-Averaged and Linear-Response CASSCF/AMOEBA formulations

Tommaso Nottoli, Lorenzo Lapi, Giacomo Londi, Filippo Lipparini, and Benedetta Mennucci

Dipartimento di Chimica e Chimica Industriale, Università di Pisa, Via G. Moruzzi 13, I-56124 Pisa, Italy

1 Additional Tables

Table S1: LR-CAS(8,8)/6-31G(d)/AMOEBA excitation energies $\mathbf{E}_{LR}$ in eV and oscillator strengths **f** for the first fourteen excited states of both @opt(GS) and @opt(LE) geometries, and fifteen excited states at the @opt(CT) geometry.

@opt(GS)		**@opt(LE)**		**@opt(CT)**	
$\mathbf{E}_{LR}$	**f**	$\mathbf{E}_{LR}$	**f**	$\mathbf{E}_{LR}$	**f**
$3.70^{\mathbf{LE}}$	0.296	$3.03^{\mathbf{LE}}$	0.286	$3.06^{\mathbf{LE}}$	0.316
4.56	0.018	4.34	0.285	4.22	0.211
4.74	0.369	4.45	0.049	4.28	0.030
5.49	0.033	5.15	0.033	5.07	0.064
6.06	0.000	5.84	0.000	5.52	0.001
6.32	0.363	5.90	0.098	5.75	0.057
6.37	0.057	6.11	0.177	$5.82^{\mathbf{CT}}$	0.004
6.75	0.118	6.53	0.105	6.10	0.039
7.03	0.003	6.93	0.846	6.12	0.000
7.28	0.286	6.97	0.002	6.33	0.077
7.29	0.535	6.99	0.050	6.60	0.350
7.46	0.292	7.12	0.113	6.75	0.013
7.53	0.000	7.46	0.234	6.82	0.004
7.64	0.001	7.50	0.002	6.86	0.563
				6.95	0.003

Table S2: 8SA-CASSCF(14,8)/6-31G(d)/AMOEBA excitation energies $\mathbf{E}_{SA}$ and their corrected values $\mathbf{E}_{SS}$ after including the state-specific corrections **SS**c, in eV, and oscillator strengths **f** at the three optimized geometries.

@opt(GS)				**@opt(LE)**				**@opt(CT)**			
$\mathbf{E}_{SA}$	**SS**c	$\mathbf{E}_{SS}$	**f**	$\mathbf{E}_{SA}$	**SS**c	$\mathbf{E}_{SS}$	**f**	$\mathbf{E}_{SA}$	**SS**c	$\mathbf{E}_{SS}$	**f**
$3.90^{\mathbf{LE}}$	-0.04	3.86	1.468	$3.12^{\mathbf{LE}}$	-0.03	3.09	0.833	$1.48^{\mathbf{CT}}$	0.04	1.52	0.008
4.65	-0.06	4.59	2.805	4.26	0.00	4.26	3.127	2.13	0.04	2.17	0.000
4.94	0.02	4.96	0.035	$5.31^{\mathbf{CT}}$	-0.34	4.97	0.025	$3.01^{\mathbf{LE}}$	-0.05	2.96	0.585
$6.18^{\mathbf{CT}}$	-0.40	5.78	0.034	5.42	-0.40	5.02	0.032	3.47	-0.09	3.38	0.002
6.29	-0.01	6.28	0.223	5.60	-0.02	5.58	0.561	3.93	-0.01	3.92	3.232
6.46	-0.43	6.02	0.016	6.07	-0.33	5.74	0.003	5.05	-0.05	5.00	0.633
7.22	0.06	7.28	0.000	7.40	-0.05	7.35	0.592	5.54	0.02	5.56	0.000

Table S3: SA-CASSCF(14,11)/6-31G(d)/AMOEBA excitation energies $\mathbf{E}_{SA}$ and their corrected values $\mathbf{E}_{SS}$ after including the state-specific corrections **SS**c, in eV, and oscillator strengths **f** at the three optimized geometries. The calculations were run with 7 states for @opt(GS) and @opt(LE) geometries, and for 6 states for the @opt(CT) geometry.

@opt(GS)				**@opt(LE)**				**@opt(CT)**			
$\mathbf{E}_{SA}$	**SS**c	$\mathbf{E}_{SS}$	**f**	$\mathbf{E}_{SA}$	**SS**c	$\mathbf{E}_{SS}$	**f**	$\mathbf{E}_{SA}$	**SS**c	$\mathbf{E}_{SS}$	**f**
$3.51^{\mathbf{LE}}$	-0.02	3.49	0.719	$2.85^{\mathbf{LE}}$	-0.01	2.84	0.651	$2.59^{\mathbf{CT}}$	-0.15	2.44	0.005
4.39	-0.05	4.34	1.775	3.97	-0.03	3.94	1.676	$2.82^{\mathbf{LE}}$	-0.02	2.80	0.658
5.50	-0.01	5.49	0.139	4.98	-0.02	4.95	0.053	3.15	-0.17	2.98	0.000
5.89	0.04	5.93	0.006	$5.41^{\mathbf{CT}}$	-0.40	5.01	0.007	3.71	-0.05	3.66	1.637
$5.99^{\mathbf{CT}}$	-0.29	5.70	0.004	5.65	0.06	5.71	0.037	4.68	-0.03	4.65	0.028
6.26	-0.43	5.83	0.009	5.70	-0.29	5.41	0.012	–	–	–	–

Table S4: TD-DFT/ωB97X-D/6-31G(d)/AMOEBA excitation energies $\mathbf{E}_{LR}$ and their corrected values $\mathbf{E}_{cLR2}$ after including the state-specific corrections **SS**c, in eV, and oscillator strengths **f** at the three optimized geometries for the first 4 excited states.

@opt(GS)				**@opt(LE)**				**@opt(CT)**			
$\mathbf{E}_{LR}$	**SS**c	$\mathbf{E}_{cLR2}$	**f**	$\mathbf{E}_{LR}$	**SS**c	$\mathbf{E}_{cLR2}$	**f**	$\mathbf{E}_{LR}$	**SS**c	$\mathbf{E}_{cLR2}$	**f**
$3.19^{\mathbf{LE}}$	-0.02	3.17	0.297	$2.71^{\mathbf{LE}}$	-0.02	2.69	0.210	$1.60^{\mathbf{CT}}$	-0.93	0.67	0.003
3.73	-0.01	3.72	0.029	3.50	-0.04	3.46	0.312	2.57	-0.98	1.59	0.001
3.83	-0.06	3.77	0.263	3.60	-0.01	3.59	0.005	$2.63^{\mathbf{LE}}$	-0.02	2.61	0.222
$4.37^{\mathbf{CT}}$	-0.71	3.66	0.004	$3.95^{\mathbf{CT}}$	-0.72	3.23	0.008	2.75	-1.00	1.75	0.001

Table S5: LR-CASSCF(8,8)/6-31G(d) gas phase excitation energies $\mathbf{E}_{LR}$ in eV and oscillator strengths **f** for the first fifteen excited states at the three optimized geometries.

@opt(GS)		**@opt(LE)**		**@opt(CT)**	
$\mathbf{E}_{LR}$	**f**	$\mathbf{E}_{LR}$	**f**	$\mathbf{E}_{LR}$	**f**
$4.07^{\mathbf{LE}}$	0.097	$3.62^{\mathbf{LE}}$	0.148	$3.65^{\mathbf{LE}}$	0.233
4.15	0.026	4.02	0.009	3.90	0.005
4.90	0.456	4.56	0.364	3.98	0.008
5.43	0.001	5.18	0.001	4.02	0.000
5.93	0.026	5.58	0.010	4.09	0.000
6.32	0.102	5.94	0.105	4.37	0.180
6.47	0.029	6.21	0.057	$4.79^{\mathbf{CT}}$	4×10^{-4}
6.58	0.199	6.24	0.032	5.38	0.073
6.68	0.150	6.41	0.206	5.52	0.032
6.73	0.044	$6.50^{\mathbf{CT}}$	0.013	5.88	0.367
6.96	0.002	6.55	0.029	6.17	0.031
6.99	0.006	6.74	0.002	6.30	0.017
$7.25^{\mathbf{CT}}$	0.004	6.96	0.001	6.35	0.000
7.32	0.281	7.04	0.209	6.63	0.000
7.47	0.073	7.24	0.088	6.73	0.001

Table S6: SA-CASSCF(14,8)/6-31G(d) gas phase excitation energies $\mathbf{E}_{SA}$ in eV and oscillator strengths at the three optimized geometries. The calculations were run at the 8SA-CAS(14,8) level for the @opt(GS) and @opt(LE) geometries, and at the 6SA-CAS(14,8) level for the @opt(CT) geometry.

@opt(GS)		**@opt(LE)**		**@opt(CT)**	
$\mathbf{E}_{SA}$	**f**	$\mathbf{E}_{SA}$	**f**	$\mathbf{E}_{SA}$	**f**
$4.33^{\mathbf{LE}}$	1.955	$3.64^{\mathbf{LE}}$	1.552	$0.60^{\mathbf{CT}}$	0.018
4.43	0.160	3.92	0.075	0.84	0.000
4.45	0.255	$4.14^{\mathbf{CT}}$	0.066	1.98	0.003
$4.67^{\mathbf{CT}}$	0.080	4.28	0.114	$3.53^{\mathbf{LE}}$	1.699
5.00	1.025	4.48	0.954	4.26	1.843
5.14	0.601	4.63	0.912		
7.04	0.000	6.29	0.001		

2 Additional Figures

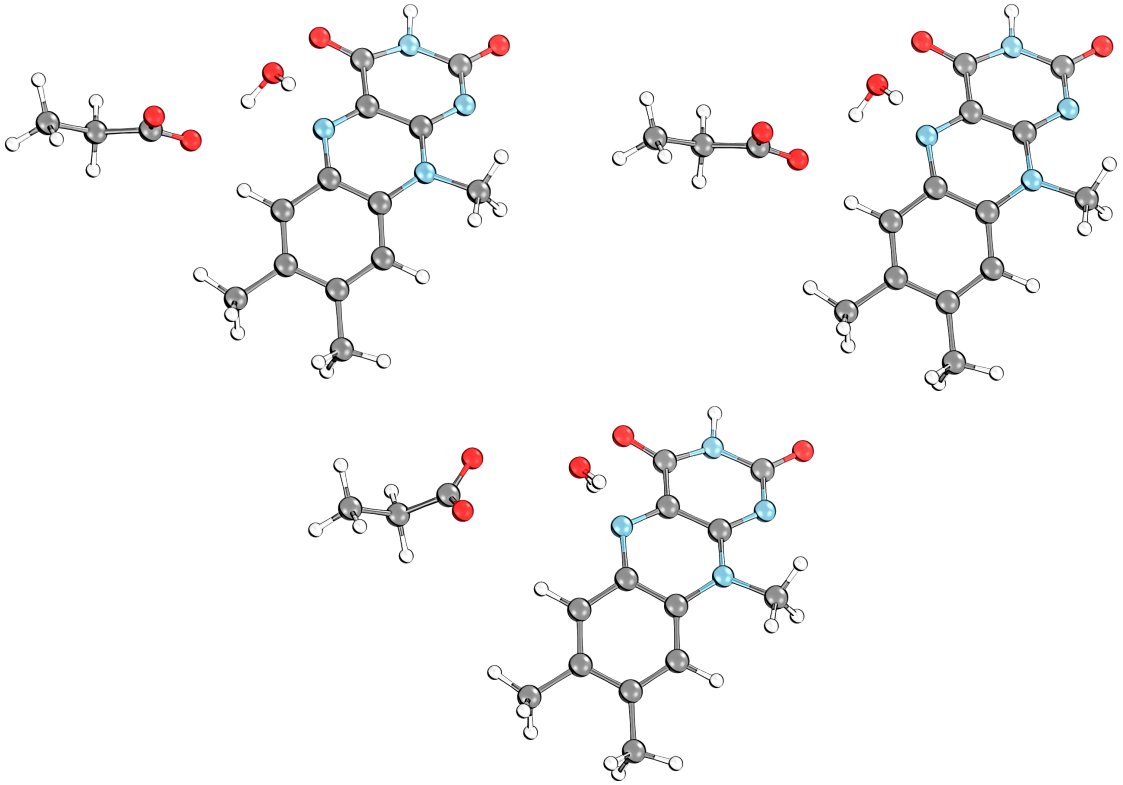

Figure S1: Ground state geometries of @opt(GS) (left), @opt(LE) (right) and @opt(CT) (bottom).

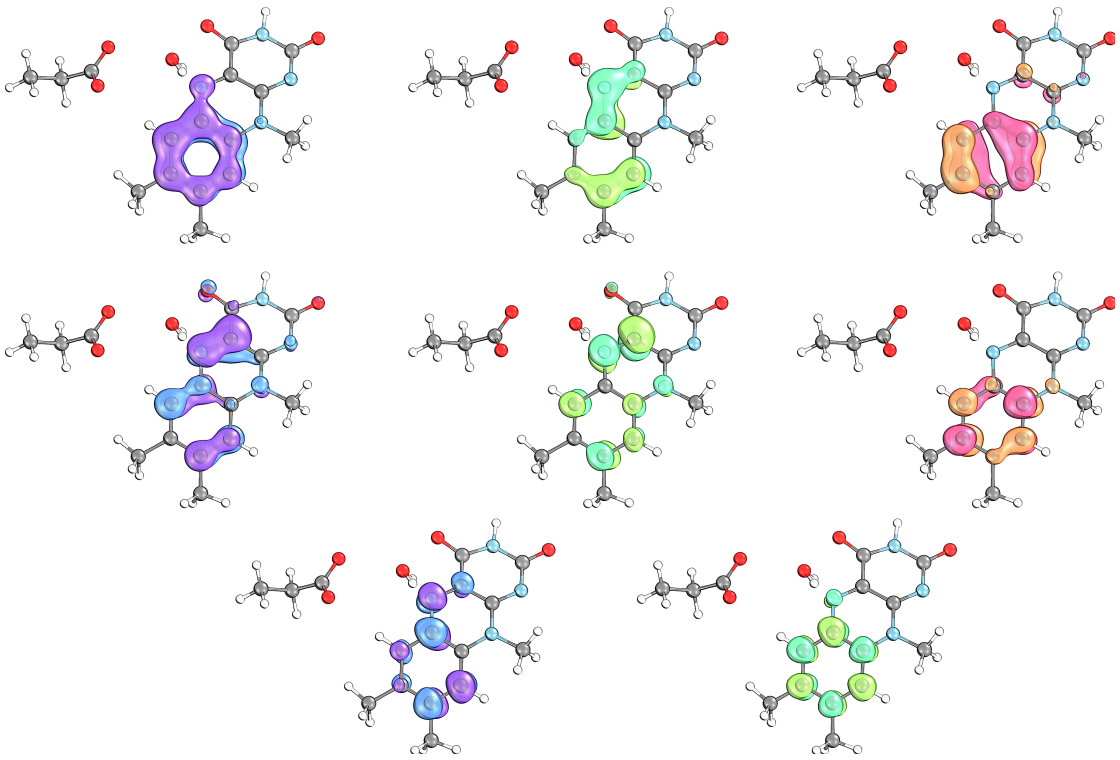

Figure S2: Converged CAS(8,8) active-space orbitals at the @opt(CT) structure, displayed in order from left to right and top to bottom. The corresponding orbitals for the @opt(GS) and @opt(LE) geometries are not shown, as they are identical to these.

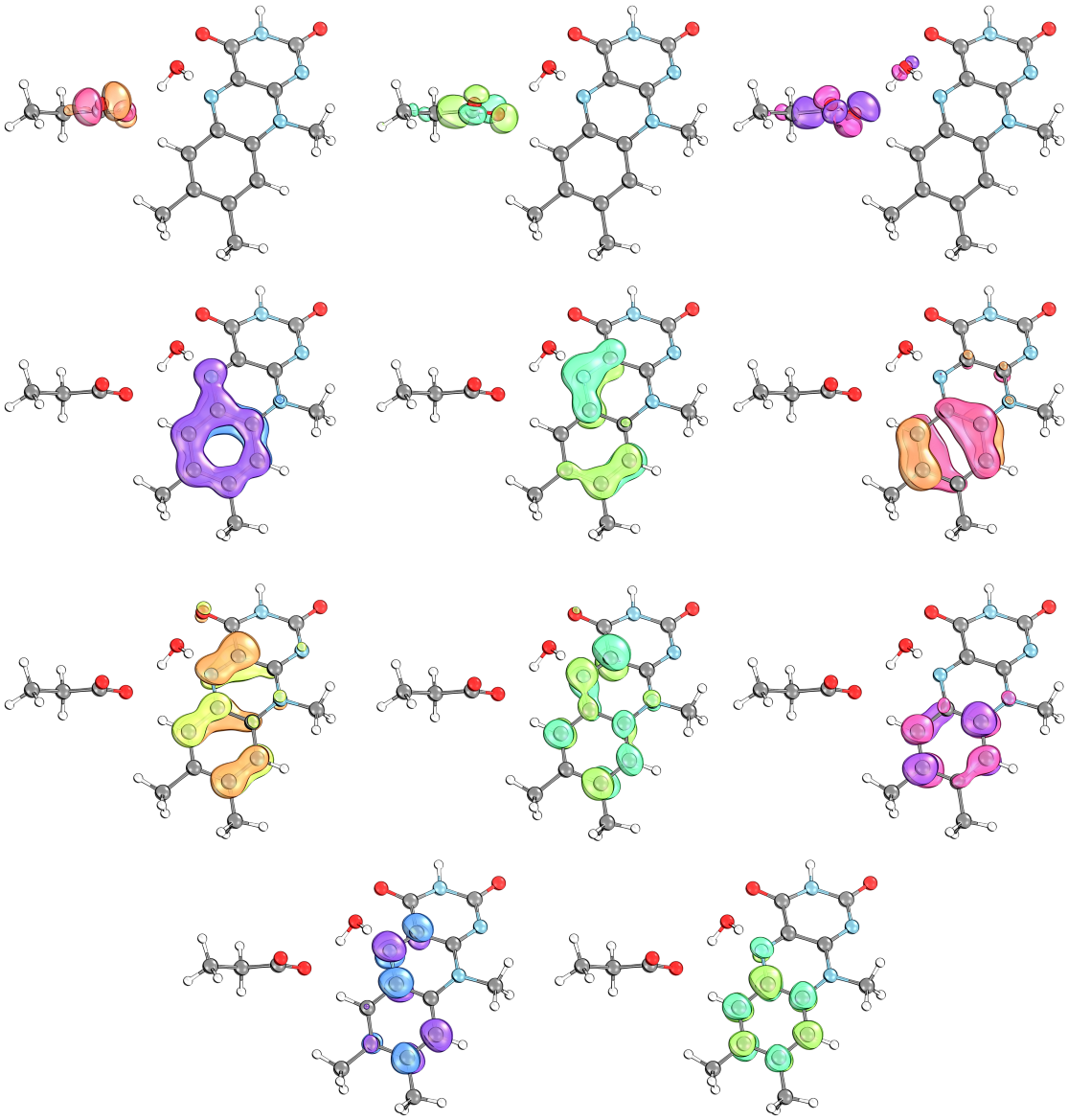

Figure S3: HOMO-6 to LUMO+3 orbitals at convergence of a CAS(8,8) ground-state calculation at the @opt(LE) structure to be used as input for subsequent 8SA-CASSCF(14,8) and 7SA-CASSCF(14,11) calculations, displayed in order from left to right and top to bottom. The pictures for the @opt(GS) and @opt(CT) are not reported since they are almost identical.

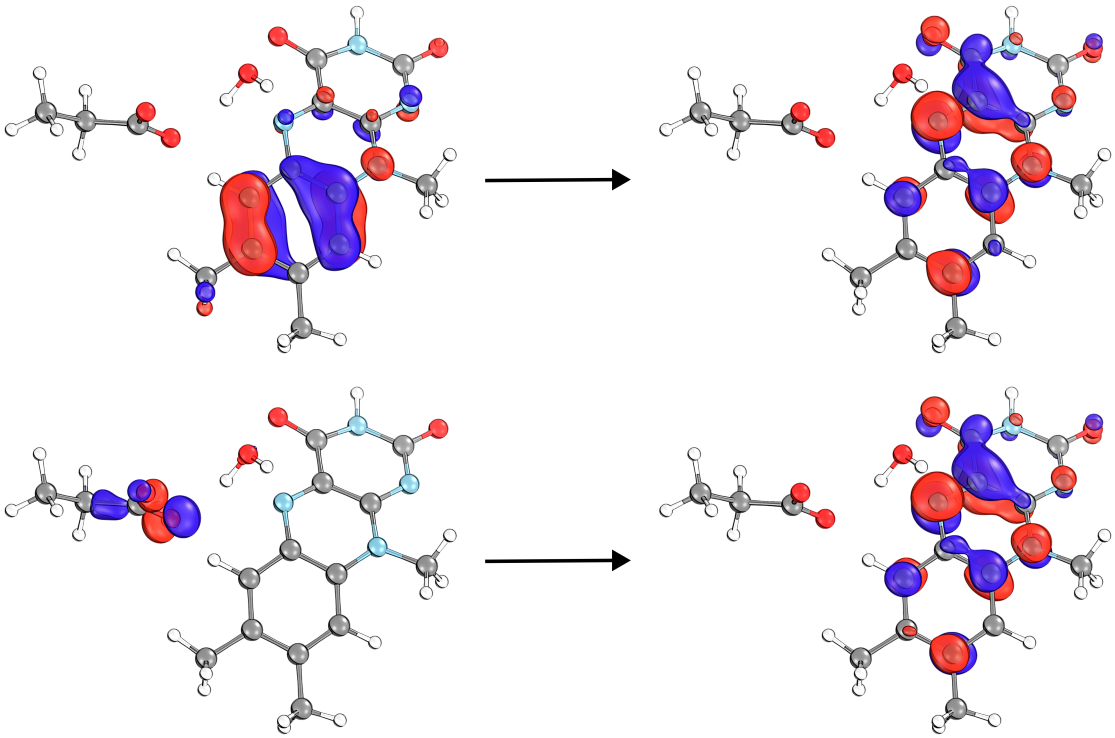

Figure S4: Natural transition orbitals of the first (top) and fourth (bottom) transitions for the @opt(LE) geometry, obtained through the SA-CAS(14,11) calculation.

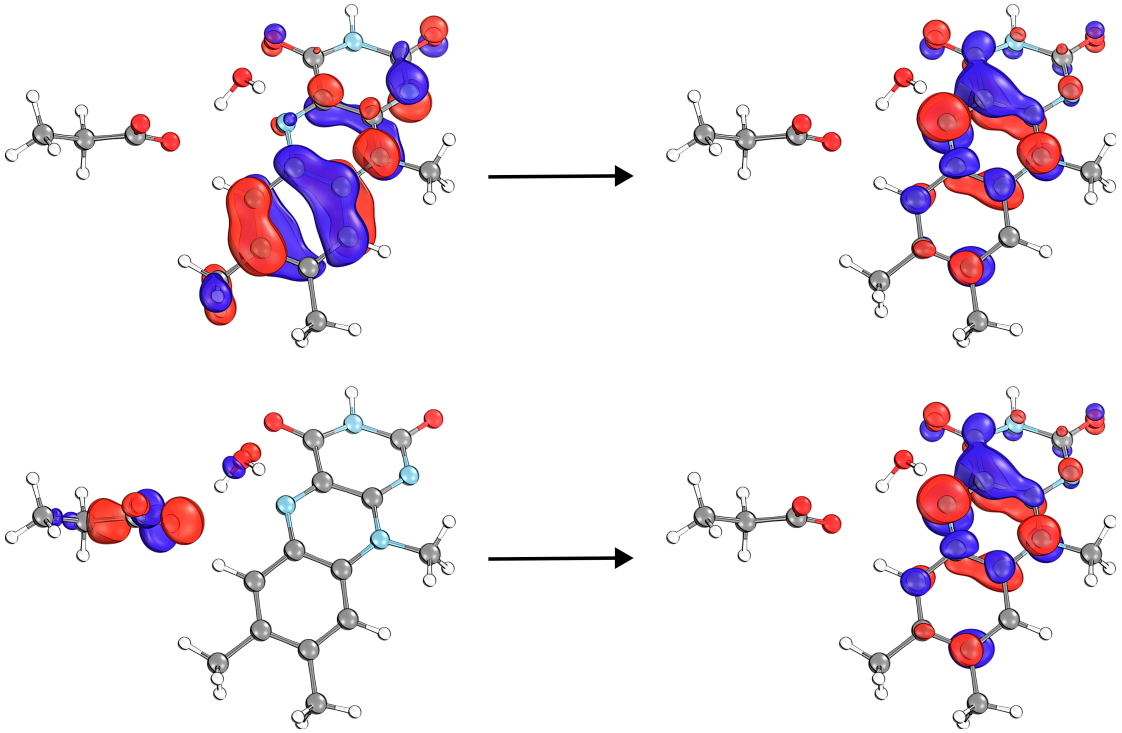

Figure S5: Natural transition orbitals of the first (top) and fourth (bottom) transitions for the @opt(GS) geometry, obtained through the SA-CAS(14,8) calculation.

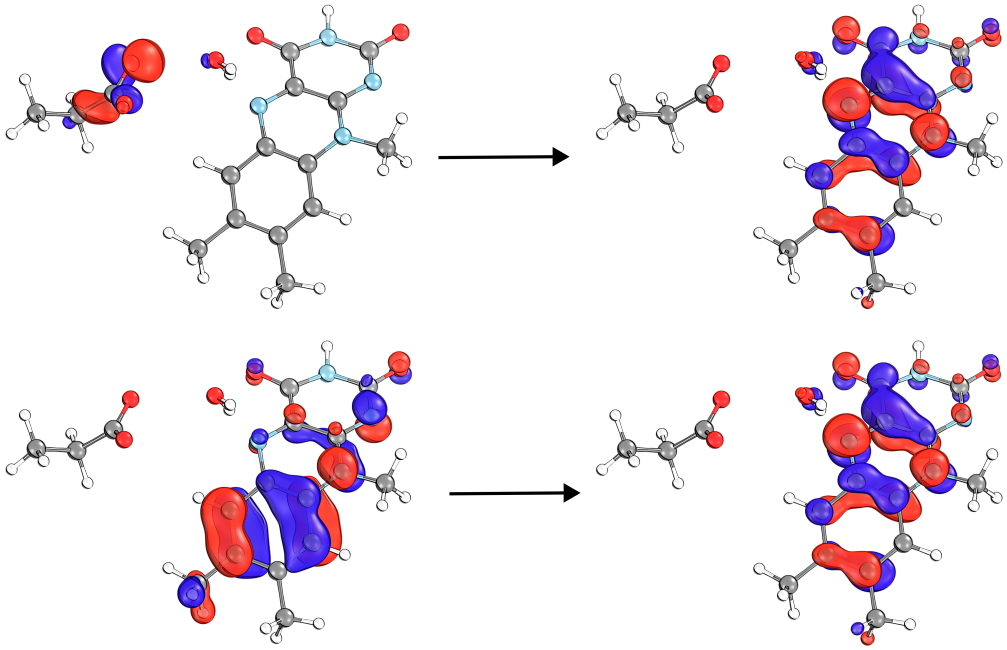

Figure S6: Natural transition orbitals of the first (top) and third (bottom) transitions for the @opt(CT) geometry, obtained through the SA-CAS(14,8) calculation.

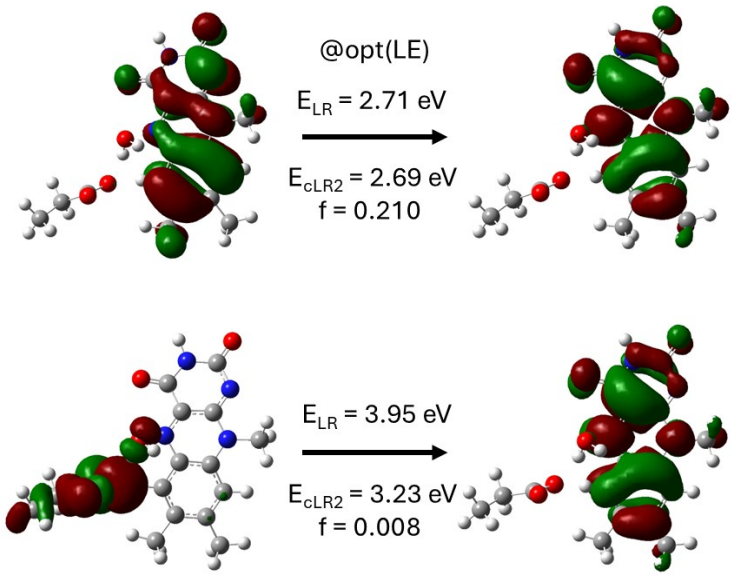

Figure S7: Hole-particle natural transition orbitals of the locally excited (LE) and the charge-transfer (CT) state for the @opt(LE) structure, as computed with TD-DFT/ωB97X-D/6-31G(d)/AMOEBA. For each excited state, the excitation energy $\mathbf{E}_{LR}$ and its corrected value $\mathbf{E}_{cLR2}$ after including the state-specific correction are reported, along with the associated oscillator strength of the transition.

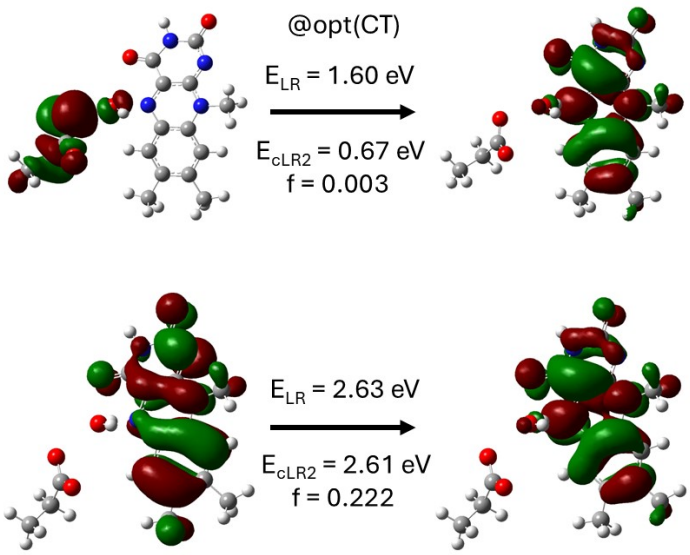

Figure S8: Hole-particle natural transition orbitals of the charge-transfer (CT) and the locally excited (LE) state for the @opt(CT) structure, as computed with TD-DFT/ωB97X-D/6-31G(d)/AMOEBA. For each excited state, the excitation energy $\mathbf{E}_{LR}$ and its corrected value $\mathbf{E}_{cLR2}$ after including the state-specific correction are reported, along with the associated oscillator strength of the transition.

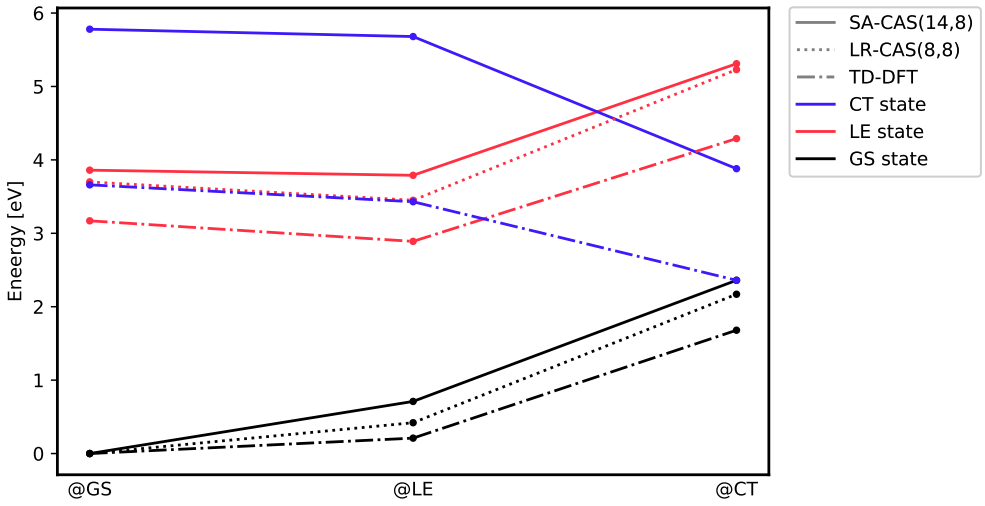

Figure S9: GS (black), LE (red), and CT (blue) energies computed on top of each geometries using as a reference the ground-state energy at the GS geometry. The linestyle denotes the level of theory: solid line for SA-CAS(14,8), dotted line for LR-CAS(8,8), and dash dotted line for TD-DFT. SA-CASSCF and TD-DFT energies include the SS correction.

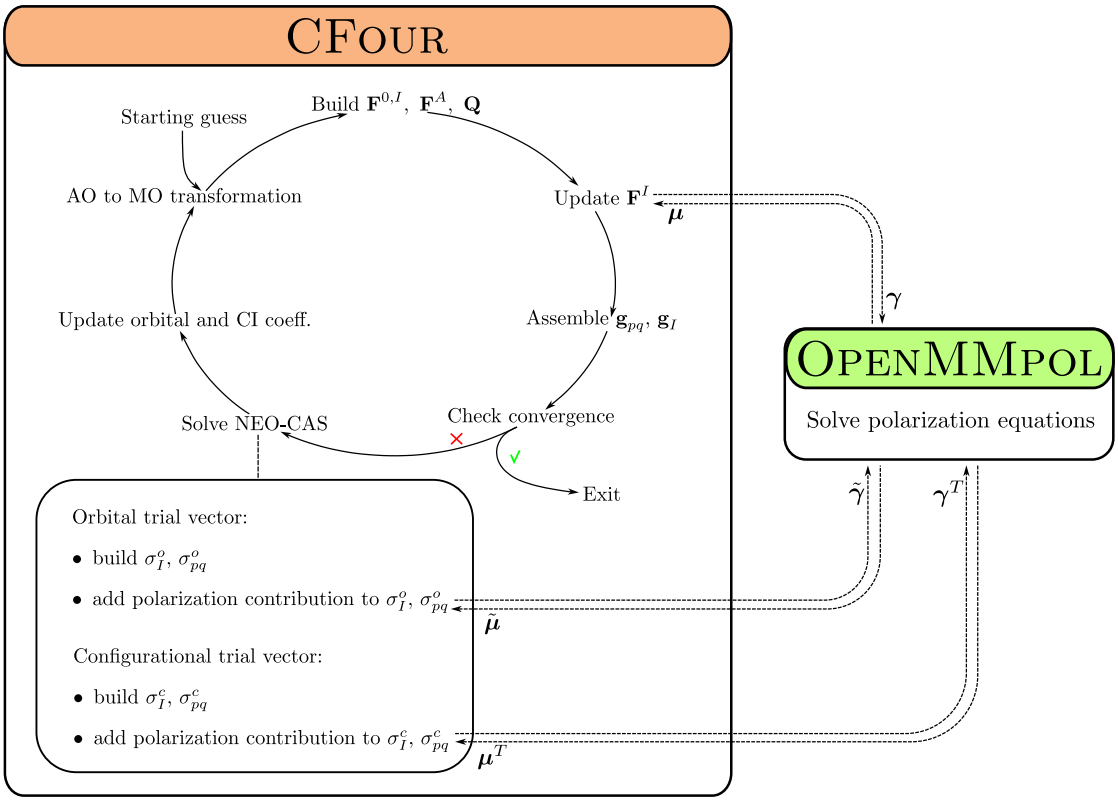

Figure S10: Workflow of the second-order CASSCF methodology implemented in CFOUR and coupled with OpenMMPol, which provides the polarizable MM environment. The linear response scheme follows a structure analogous to that of the NEO part. $\tilde{\mu}$ and μ^T are the dipoles induced by the electric field generated by the one-index transformed density matrix $\tilde{\gamma}$ and the transition density matrix γ^T, respectively.